

# Dual-layer dye-filled developer-soluble BARCs for 193-nm lithography

Jim D. Meador,<sup>a</sup> Carol Beaman,<sup>a</sup> Charlyn Stroud,<sup>a</sup> Joyce A. Lowes,<sup>a</sup> Zhimin Zhu,<sup>a</sup>  
Douglas J. Guerrero,<sup>a</sup> Ramil-Marcelo L. Mercado,<sup>a</sup> and David Drain<sup>b</sup>

<sup>a</sup>Brewer Science, Inc., 2401 Brewer Drive, Rolla, MO 65401, USA

<sup>b</sup>Missouri University of Science & Technology, 1879 Miner Circle, Rolla, MO 65401, USA

## ABSTRACT

A family of dye-filled developer-soluble bottom anti-reflective coatings (BARCs) has been developed for use in 193-nm microlithography. This new dye-filled chemical platform easily provides products covering a wide range of optical properties. The light-sensitive and positive-working BARCs use a transparent polymeric binder and a polymeric dye in a thermally crosslinking formulation, with the cured products then being photochemically decrosslinked prior to development. The cured BARC films are imaged and removed with developer in the same steps as the covering photoresist. Two dye-filled BARCs with differing optical properties were developed via a series of DOEs and then used as a dual-layer BARC stack. Lithography with this BARC stack, using a 193-nm resist, gave 150-nm L/S (1:1). A 193-nm dual-layer BARC stack (gradient optical properties) from the well-established dye-attached family of light-sensitive BARCs also gave 150-nm L/S (1:1) with the same resist. However, the latter provided much improved line shape with no scumming. The targeted application for light-sensitive dual-layer BARCs is high-numerical aperture (NA) immersion lithography where a single-layer BARC will not afford the requisite reflection control.

**Keywords:** anti-reflective, BARC, developer-soluble, dual-layer, immersion, 193-nm microlithography

## 1. INTRODUCTION

Using a bottom anti-reflective coating (BARC) under the photoresist serves to improve focus/exposure latitude, minimize both reflective notching and CD variations over topography, and solve other stray light concerns.<sup>1,2</sup> An organic BARC may be either plasma-developable (dry) or developer-soluble and thus removed in the same step as the photoresist. While the latter eliminates the reactive ion etching (RIE) step, developer-soluble BARCs do not typically provide the resolution achievable with dry BARCs. The developer-soluble products are usually aimed at noncritical applications with less demanding resolution requirements such as implant layers. However, the newer generations of 248- and particularly 193-nm developer-soluble BARCs are often light-sensitive and develop anisotropically in the same step that the photoresist is removed. These light-sensitive BARCs provide improved line shape, processing latitude, and resolution as compared to the earlier generations of polyamic acid developer-soluble products – although recent wet-developable BARCs still did not match the resolution obtainable from dry BARCs.

The expectation is that high-NA immersion lithography will enhance the resolution performance of light-sensitive developer-soluble BARCs. Immersion will be required for producing sub-50 nm microchips.<sup>3</sup> Improved resolution and increased depth of focus (DOF) can be achieved by increasing the NA of the imaging lens and by using 193-nm immersion lithography to increase the effective NA.<sup>4</sup> Unfortunately, high NAs cause light to diffract at higher angles than low NAs, which results in increased reflectance. A single-layer BARC may not provide adequate reflection control, with dual or other multilayer BARCs then becoming a preferred choice.<sup>3, 4, 5</sup> Multilayer BARCs can provide improvements in exposure latitude, DOF, and line edge roughness in addition to increased reflectance control.<sup>4</sup> This paper describes our efforts towards developing dual-layer light-sensitive developer-soluble BARCs that, when coupled with high-NA immersion technology, may give a) a possible alternative to dry BARCs for applications such as isolation/gate/contact layers and b) in some cases even a replacement for trilayer for front-end lithography. The developer-soluble BARCs increase etch budget, as the non-exposed resist is not removed during the BARC clear step.

J.D. Meador, C. Beaman, C. Stroud, J.A. Lowes, Z. Zhu, D.J. Guerrero, R.-M.L. Mercado, D. Drain, "Dual-layer dye-filled developer-soluble BARCs for 193-nm lithography," *Proceedings of SPIE*, vol. 6923, 6923-115, 2008. □

Copyright 2008 Society of Photo-Optical Instrumentation Engineers. One print or electronic copy may be made for personal use only. Systematic reproduction and distribution, duplication of any material in this paper for a fee or for commercial purposes, or modification of the content of the paper are prohibited.

Advances in Resist Materials and Processing Technology XXV, edited by Clifford L. Henderson,  
Proc. of SPIE Vol. 6923, 69232W, (2008) · 0277-786X/08/\$18 · doi: 10.1117/12.772793

The performance of 193-nm light-sensitive developer-soluble BARCs that were prepared from 1) a polymer with chemically-attached pendant chromophore and carboxylic acid moieties, 2) a multifunctional crosslinker, 3) a photoacid generator (PAG), 4) a quencher, and 5) solvents has been described in earlier papers.<sup>1, 6, 7, 8</sup> While that type of material (as a dual-layer BARC) will receive some attention in the latter section of this paper, different chemistries are now being explored with the goal being to improve developer-soluble BARC properties and performance. Thus, a new dye-filled chemical platform for 193 nm that easily provides products covering a wide range of optical properties will be highlighted and the chemistry described in a diagram. The new compositions comprise 1) a polymeric dye with acidic function, 2) an essentially transparent polymer at 193 nm with pendant carboxylic acid function, 3) a multifunctional crosslinker, 4) a PAG, 5) a photodecomposable base (PB), and 6) solvents. An aqueous solution of PB was used for this family of BARCs, as opposed to the typical types of quenchers (for example, amines). Just as for the dye-attached BARCs, these new 193-nm dye-filled BARCs are thermosetting to minimize any intermixing with the photoresist and are photochemically decrosslinked prior to development. Dye-filled KrF BARCs were discussed in a previous paper.<sup>9</sup>

To begin development of the new family of ArF dye-filled BARCs, the polymeric dye, 193-nm transparent polymer, multifunctional crosslinker, and solvents were combined (PAG and PB excluded) in a 17-specimen experimental design (DOE). The work identified many blends offering good coating quality, resistance to photoresist solvents and developer, and a wide range of 193-nm optical properties. The latter includes the refractive index  $n$  and the imaginary part of the refractive index  $k$ . Two dye-filled blends (193-nm  $k$ -values 0.2 and  $\sim 0.5$ -0.6) were then studied for BARC performance using factorial PAG/PB DOEs. The two best solutions of BARC formulations (193-nm  $k$ -values 0.20 and 0.49, respectively) were subsequently prepared, and a dual-layer stack of the BARCs with gradient  $k$ -values was tested for lithographic performance. For comparative purposes, selected lithography using dual-layer light-sensitive dye-attached BARCs (193-nm  $k$ -values of 0.19 and 0.39, respectively) is also shown in this paper.

## 2. METHODOLOGY

All BARCs described in this paper used industry-accepted solvents such as propylene glycol monomethyl ether (PGME), propylene glycol monomethyl ether acetate (PGMEA), ethyl lactate (EL), or combinations of same. The BARCs and polymer blends were all end-point filtered prior to testing. The spin-application and hot plate bake parameters varied and are described for each table of data. A Gaertner ellipsometer was used to measure film thickness of cured and stripped coatings, in all cases on a silicon substrate. The standard EL stripping test was used to assess sensitivity to photoresist solvents.<sup>10</sup> In the absence of a covering resist, the BARC post-exposure bake (PEB) parameters were 130°C for 90 seconds. The effects of 0.26 normal (N) aqueous tetramethylammonium hydroxide (TMAH) developer on both light-exposed and unexposed (dark loss) BARC coatings were measured using a 60-second puddle, a 5-second deionized water rinse, and a spin dry. Optical parameters for blends and BARCs were measured using a J.A. Woollam Co Inc. VASE<sup>®</sup>. Weight-average molecular weight ( $M_w$ ) was determined by gel permeation chromatography (GPC). Contrast curves for the 193-nm BARCs were prepared using an Oriel<sup>™</sup> DUV broadband exposure unit, with the light passing through a 248-nm bandpass filter prior to the exposure. The 193-nm exposures using a photoresist were carried out on an Amphibian<sup>™</sup> interferometer from Amphibian Systems, with scanning electron microscope (SEM) photos of cross-sectioned wafers being from a LEO 1560 from Carl Zeiss SMT Incorporated. The same 193-nm photoresist was used for all lithography and optical simulations.

## 3. RESULTS AND DISCUSSION

### 3.1 Dye-filled BARC chemistry

The dye-filled BARC formulations contain a polymeric dye with acidic function, an essentially transparent polymer with pendant carboxylic acid groups, a multifunctional crosslinker, PAG, PB, and solvents. For the initial DOE (no PAG or PB), a polymer with a linear backbone was used as the dye. For the subsequent PAG/PB DOEs and preparation of DOE-identified best solution BARCs, the dye was changed to a structurally isomeric branched polymer in order to improve compatibility with traces of water from the PB solution. The transparent polymer for the DOE blends had a weight-average molecular weight ( $M_w$ ) of about 45,200. While the composition of charged monomers/initiator/solvent and polymerization conditions remained essentially constant, the  $M_w$  for the batch of transparent polymer used for all other work was 36,700. The dye-filled BARCs are solvent-soluble until cured (crosslinked) on a hot plate, thus promising compatibility with edge bead removers (EBRs). Solvent is removed from the spin-coated BARC during the

hot plate bake step, and the crosslinker reacts with a) the acidic function on the dye and b) the carboxylic acid function on the transparent polymer, resulting in a solvent-insoluble film. An exposure with 193-nm light, followed by a PEB, regenerates the acidic function on both dye and polymer and also forms reaction by-products. Dye, polymer, and by-products are removed during the aqueous TMAH development and aqueous rinse steps, thus giving developer-solubility in the light-exposed areas. The chemistry is depicted in Figure 1.

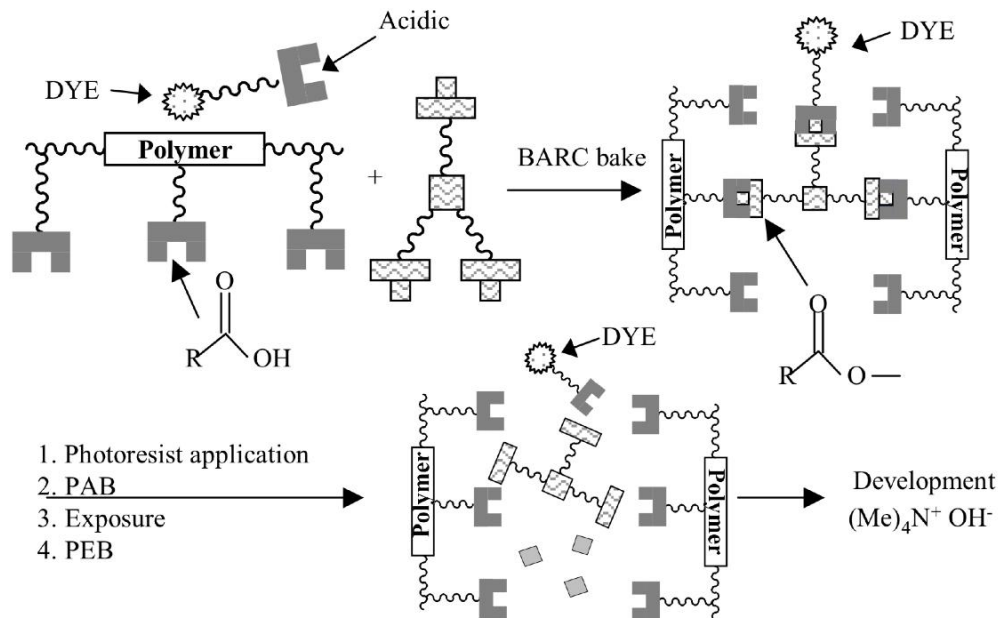


Figure 1. Graphical depiction of the BARC crosslinking and photoinduced decrosslinking process.

### 3.2 Designed experiment (i.e., blends of polymer, dye, crosslinker, and solvents)

Blends of polymer, dye, and crosslinker that gave promising film (includes optical) properties were identified. The selected blends were then optimized for BARC performance by adding PAG and PB in a second DOE. A dual-layer of DOE-identified best solution dye-filled BARCs was then to be tested for lithographic performance using a photoresist.

A simple lattice mixture design with 3 factors and 4 responses was used for the blends study. The amounts of polymer, dye, and crosslinker served as the factors. The responses were EL stripping, dark loss,  $n$ , and  $k$ . The compositions of the various blends and the blends' film properties are shown in Table I. Runs 2 and 16, 5 and 15, 6 and 11, and 7 and 13 were duplicates. A covering photoresist was not used in generating a blend's film properties. The solvent (EL) stripping test for a coating always occurs prior to the development testing. For the measurement of dark loss, there was neither light-exposure nor PEB steps. The latter procedure differs from the following PAG/PB DOEs where a PEB was now used in measuring dark loss. The 193-nm  $k$ -values varied from 0.16 to 0.56 for the 17 blends, while the refractive indices ranged from 1.46-1.60. From this first set of experiments, two blends were chosen for the desired optical properties at 193 nm: blend a (193-nm  $n/k$  of 1.56/0.18) and blend b (193-nm  $n/k$  of 1.46/0.56). The 193-nm  $k$ -values for these two blends are comparable to those reported for a dual-layer dry BARC system, i.e., 0.20 and 0.61.<sup>3</sup> For the purpose of comparing a dye-attached system, a dual-layer dye-attached BARC stack with 193-nm  $n/k$  of 1.60/0.19 and 1.63/0.39 gave very promising lithography as shown in section 3.6.

### 3.3 Optimization for 0.2 $k$ -value BARCs

To convert a blend of polymer, crosslinker, and polymeric dye with 193-nm  $k$ -value of 0.2 into an optimized photosensitive BARC, an 11-specimen two-level factorial design with five responses was run. The factors were PAG and PB. The responses are discussed in section 3.3.2. The data for the DOE, including the compositions of the BARC formulations and the measured film properties for said formulations, are shown in Table II. As may be seen, this DOE consisted of four duplicate runs (1 and 8, 2 and 7, 4 and 9, and 5 and 10) and a triplicate run (3, 6, and 11). The

75.77 grams of “Others” were comprised of 0.68 gram of transparent polymer with Mw 36,700, 0.21 gram of the branched chain polymeric dye, 0.34 gram of crosslinker, and solvents. The PB was a 23.2% (w/w) solution. The cured film thicknesses varied between 53 and 56 nm. All 11 formulations showed good resistance to the standard EL stripping test. Only PAG/PB DOE runs 5 and 10, which contained the maximum amount of PAG and minimum weight of PB solution, showed a significant (-8%) dark loss. With the exception of runs 4 and 9, all light-exposed and thermally processed BARCs were completely removed by developer. These latter two runs used the minimum weight of PAG and maximum amount of PB solution in this 0.2 k-value study. The 193-nm optical parameters were consistent for all 11 specimens: n/k 1.55-1.56/0.20-0.21.

Table I. 1) Compositions of the blends of polymer, dye, and crosslinker; and  
2) film properties for the blends.

Run #	Polymer, g	Dye, g	Crosslinker, g	Film Thickness nm <sup>a</sup>	EL Stripping or Swell <sup>b</sup>	Development Unexposed	n at 193 nm	k at 193 nm
1	0.170	0.168	0.070	39.5	+0.53%	+6.85%	1.55	0.41
2	0.102	0.120	0.164	35.6	-0.34%	+2.02%	1.53	0.39
3	0.136	0.168	0.094	37.9	-0.06%	+5.25%	1.52	0.43
4	0.259	0.120	0.070	39.8	-0.77%	+8.87%	1.56	0.26
5	0.306	0.072	0.070	38.7	-1.39%	+11.25%	1.60	0.16
6	0.102	0.072	0.211	35.3	-1.08%	+1.90%	1.50	0.29
7	0.102	0.216	0.070	39.9	+1.13%	+3.64%	1.46	0.56
8	0.238	0.096	0.094	38.9	-0.53%	+3.72%	1.56	0.22
9	0.102	0.168	0.117	37.5	0.00%	+2.36%	1.49	0.46
10	0.170	0.072	0.164	37.9	-0.10%	+1.71%	1.52	0.21
11	0.102	0.072	0.211	36.0	-0.74%	+1.43%	1.56	0.30
12	0.238	0.072	0.117	37.8	-0.28%	+0.89%	1.56	0.18
13	0.102	0.216	0.070	39.4	+2.04%	+0.67%	1.46	0.56
14	0.136	0.096	0.164	37.1	+0.82%	+1.05%	1.51	0.28
15	0.306	0.072	0.070	38.9	+0.09%	+5.14%	1.60	0.16
16	0.102	0.120	0.164	36.5	+0.97%	+1.22%	1.49	0.37
17	0.170	0.120	0.117	37.4	-72.88%	-100.00%	1.52	0.31

<sup>a</sup>Spun at 1500 rpm for 60 seconds and baked at 165°C for 60 seconds.

<sup>b</sup>(+) values indicate swelling, (-) indicate film loss.

Table II. Compositions of the 0.2 k-value BARCs and film properties for the products.

Run #	Others, g	PAG, mg	PB solution, mg	EL Stripping or Swell	Development Unexposed (with PEB)	Development Exposed <sup>b</sup> (with PEB)
1	75.77	16	8	+1.62%	-0.38%	-100.00%
2	75.77	65	133	-3.01%	-0.73%	-100.00%
3	75.77	40	70	-0.63%	-1.09%	-100.00%
4	75.77	16	140	-0.37%	-0.37%	-6.48%
5	75.77	65	9	-1.26%	-8.09%	-100.00%
6	75.77	40	71	-0.64%	-0.37%	-100.00%
7	75.77	64	133	-1.95%	-2.00%	-100.00%
8	75.77	16	9	+0.55%	-1.65%	-100.00%
9	75.77	17	140	-0.18%	-1.28%	-6.76%
10	75.78	65	10	-0.72%	-8.39%	-100.00%
11	75.77	39	74	-0.18%	-0.91%	-100.00%

<sup>a</sup>Spun at 1500 rpm for 60 seconds and baked at 160°C for 60 seconds.

<sup>b</sup>Exposed at 20 mJ/cm<sup>2</sup> with broadband light from the Oriel exposure unit.

### 3.3.1 Contrast curves for 0.2 k-value BARCs

The contrast curves for the 11 dye-filled PAG/PB DOE specimens using an Oriel DUV broadband light source are shown in Figure 2. The BARC films were cured at 160°C for 60 seconds, with their PEB being at 130°C for 90 seconds. The light passed through a 248-nm bandpass filter prior to exposing the BARCs.

Reproducibility of contrast curves for each of the four duplicates and also for the triplicate was good. The dose-to-clear ( $E_0$ ) line up well with the weight ratios of PAG to PB solution. Thus, the higher PAG/PB solution weight ratios required less energy for exposure-to-clear. Runs 5 and 10, containing the highest weight of PAG and lowest weight of PB solution, clear with  $\sim 4.5$  mJ/cm<sup>2</sup> exposure. Other than runs 4 and 9, which contained the lowest weight ratio PAG to PB solution, they all cleared completely.

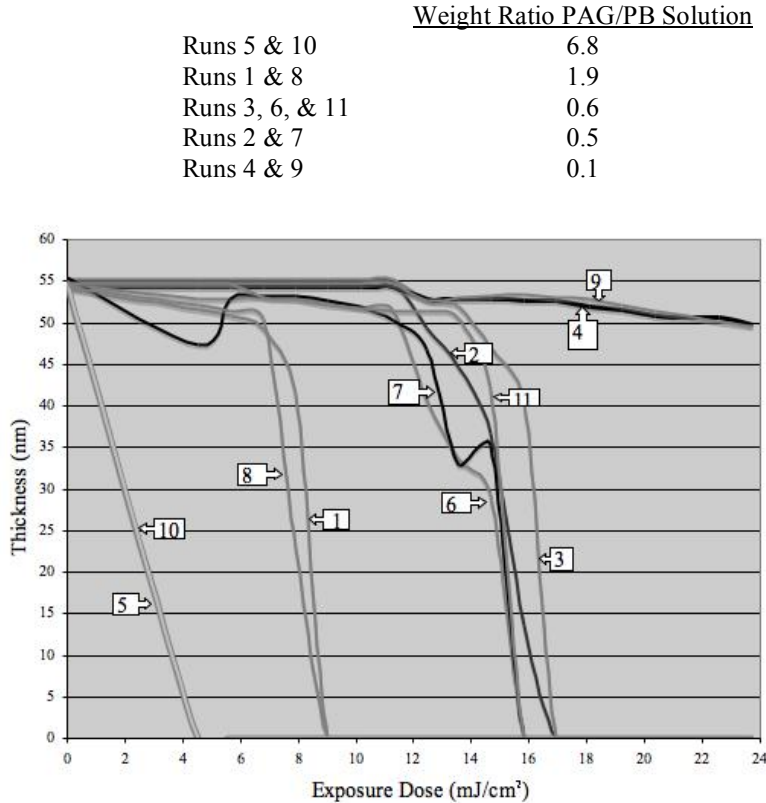


Figure 2. Contrast curves for the eleven 0.2 k-value DOE specimens.

### 3.3.2 Optimized 0.2 k-value BARC

The responses to the design were a) EL stripping, b) dark loss, c) development, d)  $E_0$ , and e) slope of the contrast curve. The slope takes into account start of development to BARC clear. The analysis gave the following conclusions:

#### Responses to the Design

- a) EL stripping
- b) dark loss
- c) development
- d)  $E_0$
- e) slope of the contrast curve

#### Significant Factors

- PAG and PB are the significant factors
- PAG, PB, and PAG/PB interactions are significant
- PAG, PB, and PAG/PB interactions are significant
- PAG, PB, and PAG/PB interactions are significant
- PAG, PB, and PAG/PB interactions are significant

The DOE-identified best solution was to use 37.3 mg of PAG and 8.6 mg of PB solution (23.2% solids) with 75.77 grams of “Others.” This formulation became BARC V. DOE software analysis predicted properties were EL stripping: +0.18%, dark loss: -4.13%, development: -100%,  $E_0$ : 7.0 mJ/cm<sup>2</sup>, and slope: 14.0. The experimental product (V) was prepared and characterized, with the film properties results shown in Table III. A new batch of PB solution was used in

preparing formulation V, with a solids content of only 21.9%. The measured  $E_0$  for this best solution 0.2 k-value formulation was  $4.6 \text{ mJ/cm}^2$ , i.e., lower than predicted.

Table III. Properties of BARC V.

Film Thickness, nm <sup>a</sup>	EL Stripping or Swell	Development Unexposed (with PEB)	Development Exposed <sup>b</sup> (with PEB)	n at 193 nm	k at 193 nm
54.8	-0.64%	-1.05%	-100%	1.55	0.20

<sup>a</sup>Spun at 1500 rpm for 60 sec and baked at 160°C for 60 seconds.

<sup>b</sup>Exposed at  $40 \text{ mJ/cm}^2$  with broadband light from the Oriel exposure unit.

### 3.4 Optimization for 0.5 k-value BARCs

To convert the blend of transparent polymer, crosslinker, and branched polymeric dye with 193-nm k-value of 0.56 (i.e., this k-value came from the linear chain polymer dye) into an optimized BARC, the same 11-specimen two-level factorial design PAG/PB DOE with five responses was run. The data for the DOE, including the compositions of the BARC formulations and the measured film properties for the formulations, are shown in Table IV. The 75.77 grams of “Others” was comprised of 0.32 gram of transparent polymer with Mw 36,700, 0.68 gram of the branched chain polymeric dye, 0.22 gram of crosslinker, and solvents. The PB solution contained 23.2% solids. The cured film thicknesses varied between 52 and 55 nm. None of the compositions seemed to show excessive susceptibility to the EL stripping test. Dark loss was high for runs 5 and 10 (duplicates with highest PAG/PB solution weight ratio) and 1 and 8 (duplicates with moderately high PAG/PB solution weight ratio). Runs 4 and 9, which used the lowest PAG to PB solution weight ratio, displayed minimal development in developer, which is not so surprising. However, the mediocre development for runs 1 and 8 was not at all expected. There is some inconsistency for this set of data. The 193-nm n-values of 1.41 to 1.48 and the 193-nm k-values of 0.47 to 0.50 were relatively consistent, although possibly lower than expected from the original blends study. A possible reason for this may be the use of the branched isomer in this study as opposed to the linear polymer used in the blends study.

Table IV. Compositions of the 0.5 k-value BARCs and film properties for the products.

Run #	Others, g	PAG, mg	PB solution, mg	EL Stripping or Swell	Development Unexposed (with PEB)	Development Exposed <sup>b</sup> (with PEB)
1	75.77	16	8	+4.24%	-6.59%	-70.3%
2	75.77	64	133	-0.27%	-5.26%	-100.00%
3	75.77	41	71	-2.04%	-0.76%	-100.00%
4	75.77	16	134	+0.66%	-1.31%	-4.86%
5	75.77	64	9	-0.56%	-6.36%	-100.00%
6	75.77	40	72	+2.44%	-3.48%	-100.00%
7	75.77	64	133	-0.72%	-2.58%	-100.00%
8	75.77	16	9	+3.67%	-8.01%	-70.4%
9	75.77	16	138	+1.88%	-3.68%	-7.00%
10	75.78	64	9	+0.46%	-7.04%	-100.00%
11	75.77	40	75	+2.50%	-4.18%	-100.00%

<sup>a</sup>Spun at 1500 rpm for 60 sec and baked at 160°C for 60 seconds.

<sup>b</sup>Exposed at  $20 \text{ mJ/cm}^2$  with broadband light from the Oriel exposure unit.

#### 3.4.1 Contrast curves for 0.5 k-value BARCs

The contrast curves for the eleven 0.5 k-value dye-filled BARC specimens are shown in Figure 3. The exposure light was filtered through a 248-nm bandpass, with the source being the Oriel DUV broadband instrument. BARC cure and PEB parameters were as described in sections 2 and 3.3.1. Unlike the 0.2 k-value BARCs, there was not always good  $E_0$  agreement for duplicate specimens. For example, duplicate runs 2 and 7 have very different  $E_0$ s. Additionally  $E_0$  did not correlate very well with the weight ratios of PAG/PB solution.

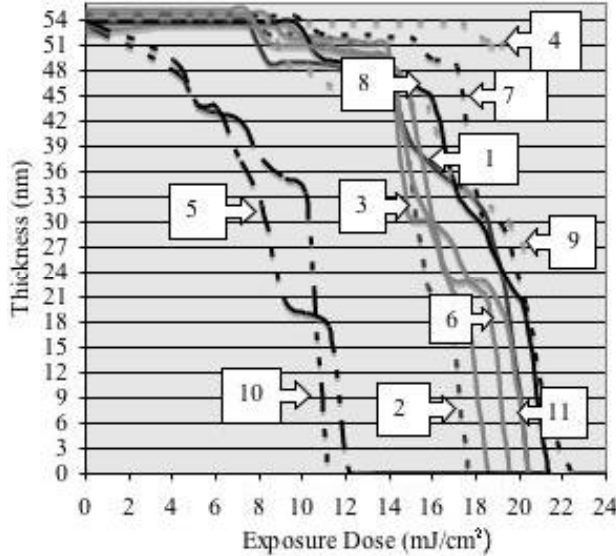


Figure 3. Contrast curves for the eleven 0.5 k-value DOE specimens.

### 3.4.2 Optimized 0.5 k-value BARC

Analysis yielded the following conclusions:

#### Responses to the Design

- a) EL stripping
- b) dark loss
- c) development
- d)  $E_0$
- e) slope of the contrast curve

#### Significant Factors

- PAG is the only significant factor
- PAG, PB, and PAG/PB interactions are significant
- PAG, PB, and PAG/PB interactions are significant
- PAG, PB, and PAG/PB interactions are significant
- PAG, PB, and PAG/PB interactions are significant

The optimized solution called for using 64.6 mg of PAG, 8.6 mg of 23.2% solids PB solution, and 75.77 grams of "Others." This formulation became BARC W. The predicted responses were EL stripping: -1.32%, dark loss: -3.45%, development: -100%,  $E_0$ : 10.7 mJ/cm<sup>2</sup>, and slope: 5.37. BARC W was prepared and the properties measured. The PB solution used for formulation W contained 21.9% solids. The  $E_0$  for the optimized 0.5 k-value formulation was 5.75 mJ/cm<sup>2</sup>. Just as for the 0.2 k-value computer-recommended BARC V, there was not very good agreement between predicted and measured  $E_0$ . The BARC properties are shown in Table V.

Table V. Properties of BARC W.

Film Thickness, nm	EL Stripping or Swell	Development Unexposed (with PEB)	Development Exposed <sup>b</sup> (with PEB)	n at 193 nm	k at 193 nm
54.6	-0.92%	-7.25%	-100%	1.47	0.49

<sup>a</sup>Spun at 1500 rpm for 60 seconds and baked at 160°C for 60 seconds.

<sup>b</sup>Exposed at 20 mJ/cm<sup>2</sup> with broadband light from the Oriel exposure unit.

### 3.5 Lithography using the dual-layer dye-filled BARCs V on W

Optical simulations were performed with an in-house simulator<sup>11</sup> to generate contour maps of top and bottom BARC thicknesses as shown in Figure 4. These maps show substrate reflectivity and UV distribution relative to resist exposure dosage. BARC V (193-nm n/k 1.55/0.20) and BARC W (193-nm n/k 1.47/0.49) were used as upper and lower BARCs, respectively. The thicknesses of 20 nm for the top BARC and 28 nm for the bottom BARC, shown by a white dot in each of the Figure 4 contour maps, were selected for the initial lithography test. The bottom BARC thickness was measured on silicon, with the top BARC thickness calculated from a measurement of the composite BARC thickness on silicon. This procedure was used for all lithography in this paper. The stack provided a simulated BARC exposure of

0.52, with reflectivity of 0.9% using a silicon substrate and the standard resist. The lithography data for this configuration are shown in Figure 5, as SEM photos of cross-sections. Three different exposure times were used, i.e., 1.6, 1.7, and 1.8 seconds. While the results were fair, in all cases there was scum between the lines and a flare at the base of resist lines. These are 150-nm L/S (1:1). The experimental parameters for all 193-nm lithography described in this paper using the Amphibian interferometer instrument are given below:

BARC bakes	160°C for 60 seconds
Thickness of photoresist	130 nm as measured on silicon, after the PAB
PAB for resist on the BARC stack	110°C for 60 seconds
Exposure times	the times are shown below the SEM photos
PEB for resist and the BARC stack	110°C for 60 seconds
Development	0.26N TMAH for 45 seconds

A possible optimization iteration for these two BARCs is to increase BARC exposure to clear the footing and scum. The proposed thicknesses are shown by a black dot in each of the maps, i.e., about 31 nm of BARC V and 24 nm of BARC W. These respective thicknesses will give a higher BARC exposure of 0.58, with 1.8% reflectivity on a silicon substrate using the standard 193-nm resist.

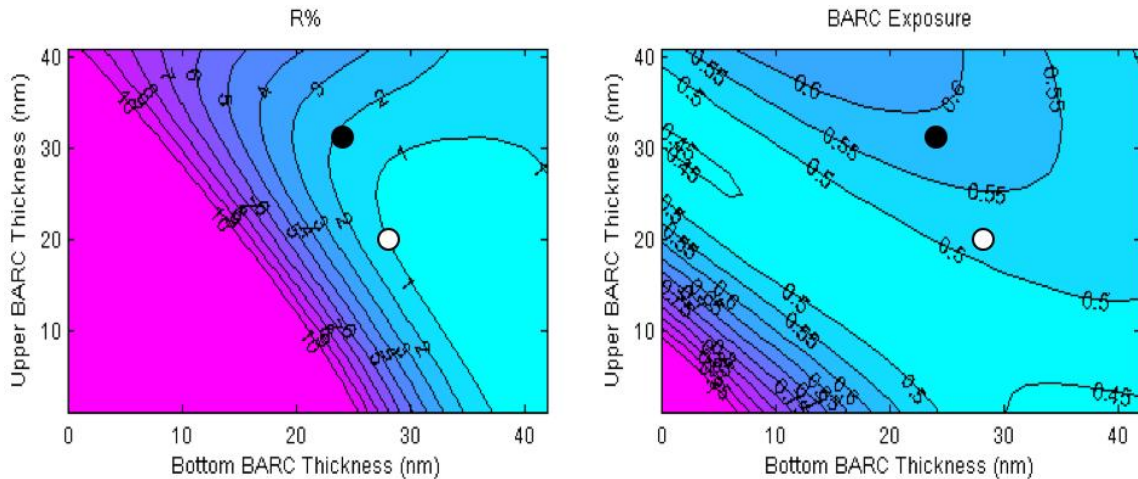
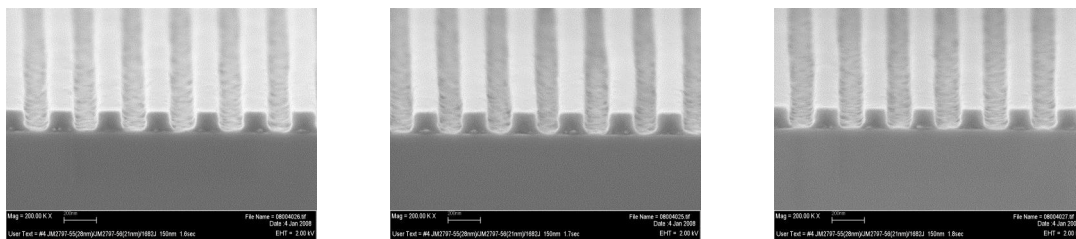


Figure 4. Contour maps for upper and lower BARC thicknesses for dye-filled BARCs V on W: a) percent reflectivity and b) average BARC exposure relative to resist exposure.



Exposure: 1.6 seconds

Exposure: 1.7 seconds

Exposure: 1.8 seconds

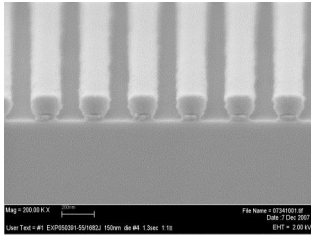
Figure 5. Lithography using dual-layer dye-filled BARCs V (20 nm) on W (28 nm).

### 3.6 Lithography using light-sensitive dye-attached BARCs EXP05039I, X, and Y

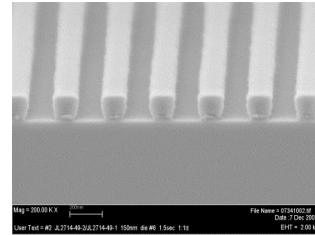
While the dual-layer dye-filled BARC chemistry may give improved lithography with additional study, the light-sensitive dye-attached BARC chemistry was used to establish promise for dual-layer developer-soluble BARCs. Figure 6 shows lithography using a 193-nm resist with a) a single layer of 193-nm light-sensitive BARC EXP05039I at 56-nm film thickness and b) two applications of EXP05039I, giving a 55-nm composite. Film thicknesses for the two



applications were about 20 nm (bottom layer) and 35 nm (top layer). This was a model study, with both BARC bakes at 160°C for 60 seconds. The SEM photos of cross-sections for the single application (Example a) show that the 150-nm lines (1:1 L/S) are underexposed and also undercut or pinched at their base. The 150-nm lines (1:1 L/S) for Example b are much improved and show only a small amount of undercutting. While there are concerns for dual-layer developer-soluble BARCs, such as 1) component leaching from the bottom BARC during application of the top BARC and 2) a double bake of the bottom BARC, a clearly-defined problem was not identified from this study with EXP05039I. This was, of course, only one comparison of a) a single BARC application versus b) two applications of same BARC.



56-nm of EXP05039I  
Exposure: 1.3 seconds  
Example a - single application



35-nm of EXP05039I on 20-nm EXP05039I  
Exposure: 1.5 seconds  
Example b - two applications

Figure 6. Lithography using BARC EXP05039I: a) single layer application and b) dual-layer applications.

Two different dye-attached BARCs, X and Y, with 193-nm n/k of 1.60/0.19 and 1.63/0.39 were then studied for lithography in a dual-layer stack using a 193-nm photoresist. BARC X was applied onto BARC Y, with the respective thicknesses being 31 nm and 22 nm. The contour maps of a) % reflectivity and b) BARC exposure for the stack, using the 193-nm resist, are shown in Figure 7. The white dot in Figure 7 shows the thicknesses initially selected for lithography (see photos in Figure 8). The % reflectivity was 4.2, with BARC exposure being 0.65. The black dot shows the thicknesses (13-nm X and 24-nm Y) selected for a second litho trial (see Figure 9) with the same two BARCs and resist. The reflectivity for this latter case was 3.9%, with BARC exposure being only 0.5. The second trial gave more scum (see Figure 9), as might be expected from the lower BARC exposure.

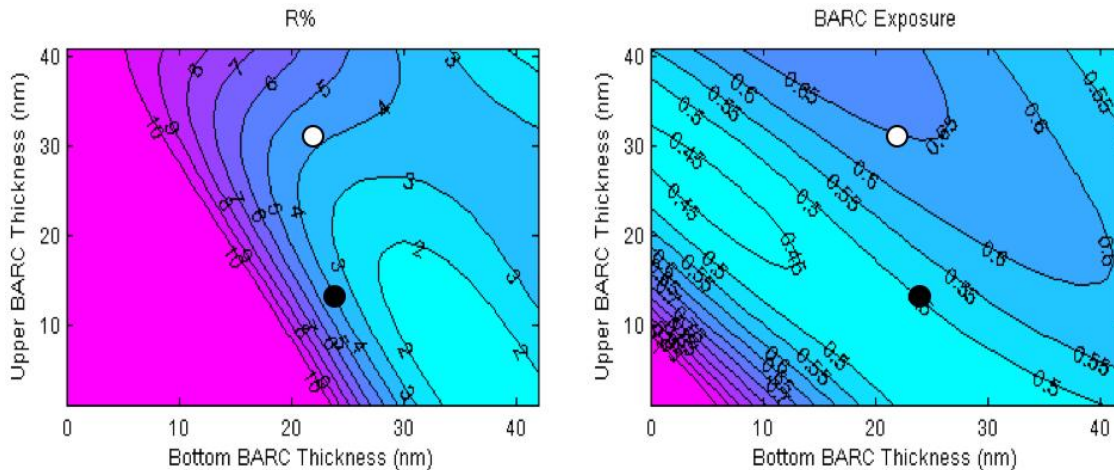


Figure 7. Contour maps for upper and lower BARC thicknesses for X and Y: a) percent reflectivity and b) average BARC exposure relative to resist exposure.

Figure 8 shows the SEM photos for BARC X (31 nm) on BARC Y (22 nm) using a 193-nm photoresist. The 150-nm L/S (1:1) with 1.8- and 1.9-second exposures were very good. 90-nm L/S (1:1) were exposed with same dual-layer BARCs (31-nm X on 22-nm Y) and resist, but the pattern did not clear before lift-off.

Figure 9 shows SEM photos for the same two dye-attached BARCs and resist at different BARC thicknesses, i.e., 13 nm of BARC X on 24 nm of product Y. In this latter example, scum between the lines was a problem. A longer exposure than 1.8 seconds might minimize the scumming issue for this BARC stack.

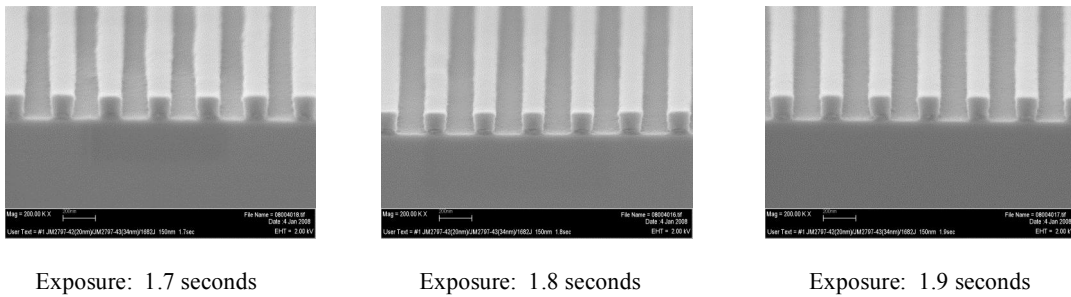


Figure 8. Lithography using dual-layer dye-attached BARCs X (31 nm) on Y (22 nm).

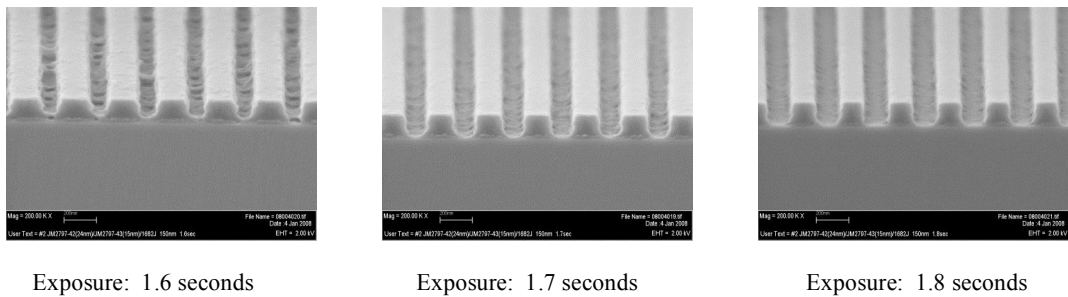


Figure 9. Lithography using dual-layer dye-attached BARCs X (13 nm) on Y (24 nm).

## CONCLUSIONS

This paper described a strategy for BARC development using DOEs as a tool, as well as the progress to date in preparing dual-layer dye-filled developer-soluble products for use in 193-nm lithography. A light-sensitive dye-filled BARC composite with  $n/k/t$  of 1.55/0.20/20 nm (top layer) and 1.47/0.49/28 nm (bottom layer) has given 150-nm L/S (1:1), although there was some scum between the lines. The use of light-sensitive dye-attached developer-soluble products has provided quicker progress towards dual-layer BARC usage. A best case for the latter was with dual-layer BARCs having  $n/k/t$  of 1.60/0.19/31 nm (top layer) and 1.63/0.39/22 nm (bottom layer). This stack gave very good results for 150-nm L/S (1:1). The L/S resolution must be improved for successful high-NA immersion applications.

## ACKNOWLEDGMENTS

Brewer Science’s Analytical Services Team and SEM Team are thanked for their valued contributions to this study. April Evers, Jamie Storie, Brian Davis, Galya Stoeva, Mariya Nagatkina, and Trisha May are acknowledged from the former group. John Thompson, Denise Howard, and Eric Stewart provided the important SEM results.

## REFERENCES

1. Xie Shao, Alice Guerrero, and Yiming Gu, “Wet-Developable Organic Anti-Reflective Coatings for Implant Layer Applications,” *SEMICON China 2004 SEMI Technology Symposium*, pp. 1-9, March 17, 2004, [www.brewerscience.com/arc\\_news/arc\\_publications.html](http://www.brewerscience.com/arc_news/arc_publications.html).
2. Jim Meador, Carol Beaman, Joyce Lowes, Carlton Washburn, Ramil Mercado, Mariya Nagatkina, and Charlyn Stroud, “Development of 193-nm wet BARCs for implant applications,” *Proc. SPIE*, 6153, pp. 854-863, 2006.

3. Zhong Xiang, Hong Zhuang, Hengpeng Wu, Jianhui Shan, Dave Abdallah, Jian Yin, Salem Mullen, Huirong Yao, Eleazar Gonzalez, and Mark Neisser, "Organic ArF Bottom Anti-Reflective Coatings for Immersion Lithography," *Proc. SPIE*, 6519, pp. 651929-1-651929-10, 2007.
4. James B. Claypool, Marc Weimer, Vandana Krishnamurthy, Wendy Gehoel, and Koen van Ingen Schenau, "New advanced BARC materials for ultra-high NA applications," *Proc. SPIE*, 5753, pp. 679-689, 2005.
5. H. L. Chen, W. C. Chao, F. H. Ko, T. C. Chu, and T. Y. Huang, "Novel bilayer bottom antireflective coating structure for high-performance ArF lithography applications," *J. Microlithography, Microfabrication, and Microsystems*, 1, No. 1, pp. 58-62, April 2002.
6. Douglas J. Guerrero, Ramil Mercado, Carlton Washburn, and Jim Meador, "Photochemical Studies on Bottom Anti-Reflective Coatings," *J. Photopolym. Sci. and Technol.*, 19, No. 3, pp. 343-347, 2006.
7. Carlton Washburn, Alice Guerrero, Ramil Mercado, Douglas Guerrero, and Jim Meador, "Process development for developer-soluble bottom anti-reflective coatings (BARCs)," *INTERFACE 2006: Proceedings of the 43<sup>rd</sup> Microlithography Symposium*, October 29-31, 2006.
8. Carlton Washburn, Ramil Mercado, Douglas Guerrero, Jim Meador, "Controlling CD and process window limits for implant patterning," *Solid State Technology*, 49, No. 10, pp. 53-56, 2006.
9. Ramil-Marcelo L. Mercado, Joyce A. Lowes, Carlton A. Washburn, and Douglas J. Guerrero, "A novel approach to developer-soluble anti-reflective coatings for 248-nm lithography," *Proc. SPIE*, 6519, pp. 65192X-1-65192X-10, 2007.
10. Jim D. Meador, Doug Holmes, William L. DiMenna, Mariya Nagatkina, Michael Rich, Tony D. Flaim, Randy Bennett, and Ichiro Kobayashi, "193-nm Multilayer Imaging Systems," *Proc. SPIE*, 5039, pp. 948-957, 2003.
11. Zhimin Zhu, Emil Pisconi, Kevin Edwards and Brian Smith, "Reflection control in hyper-NA lithography", *Proc. SPIE*, 6924-163, 2008.